Supporting Information

Mandal *et al.* 10.1073/pnas.0807557106

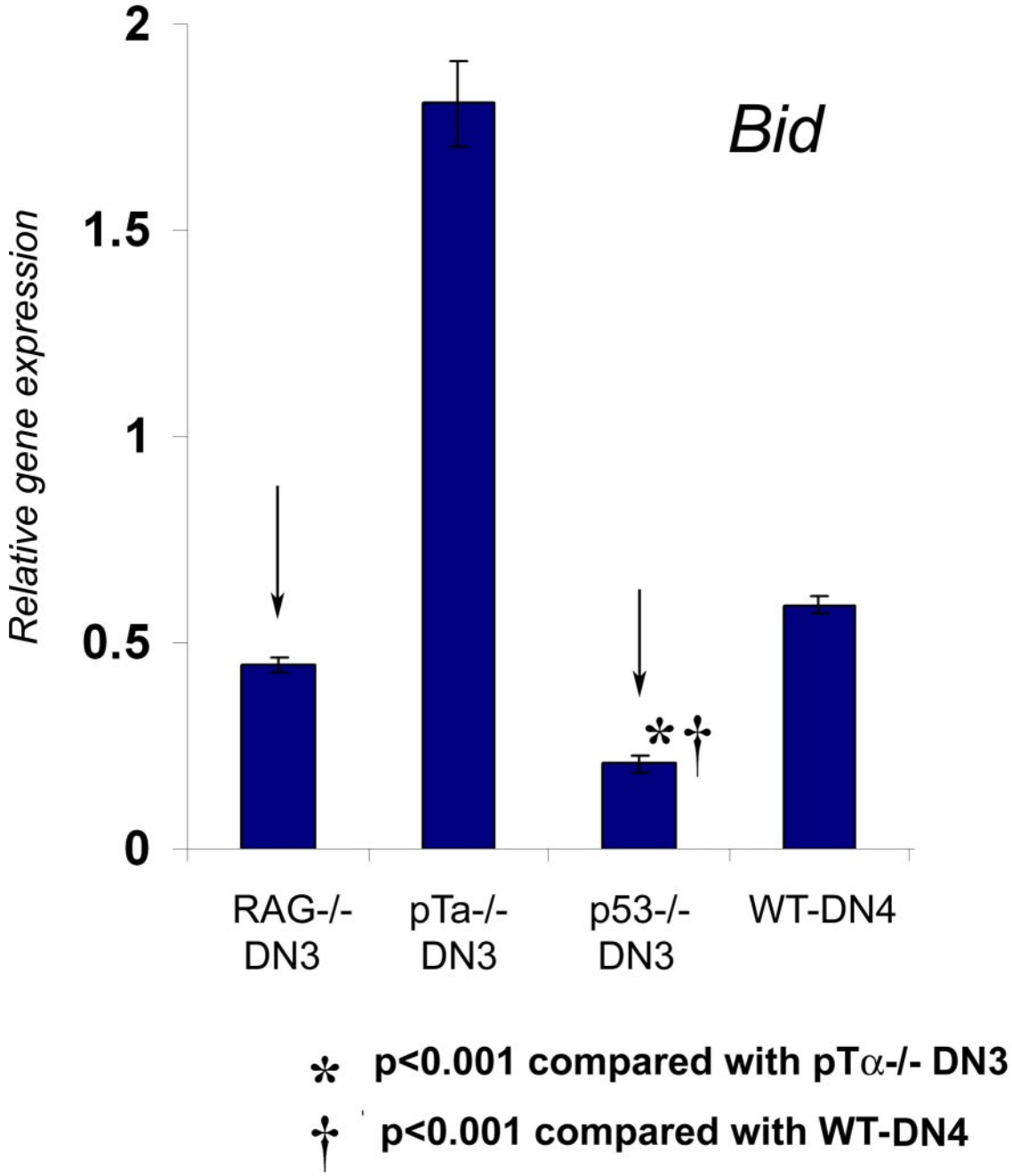

Fig. S1. Deletion of p53 silences Bid expression in thymocytes qRT-PCR by using Flow-sorted DN3 and DN4 cells from Rag-1$^{-/-}$, pTa$^{-/-}$, p53$^{-/-}$, and wild-type mice.

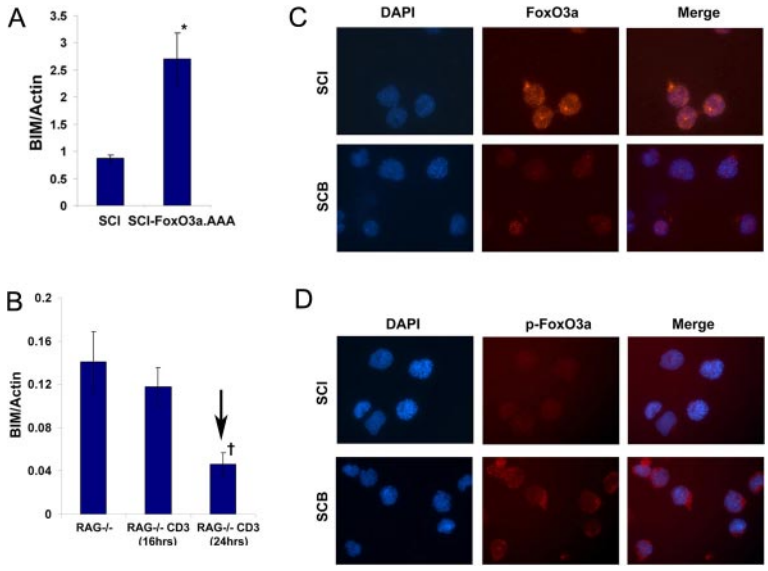

Fig. S2. Control of Foxo3a activation by the pre-T cell receptor (TCR). (*A*) Induction of Bim expression in response to Foxo3a activation via overexpression of Foxo3a mutant (FoxO3.AAA). *, $P < 0.001$. (*B*) Bim expression in total thymocytes purified from anti-CD3 injected Rag-$1^{-/-}$ mice. **, $P < 0.01$. (*C* and *D*) Immunofluorescence staining showing FoxO3a and phospho-FoxO3a expression and localization in the indicated cell lines. The data are representative of 3 independent experiments.

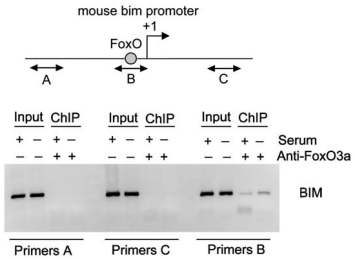

Fig. S3. Bim expression is directly controlled by Foxo3a. (*A*) Foxo3a ChIP assay in pre-TCR-deficient SCIET27 cells. The location of the primers on the mouse BIM promoter is presented schematically. Induction of Foxo3a binding, in response to serum starvation of SCIET27 cells. Data are representative of 2 independent experiments.

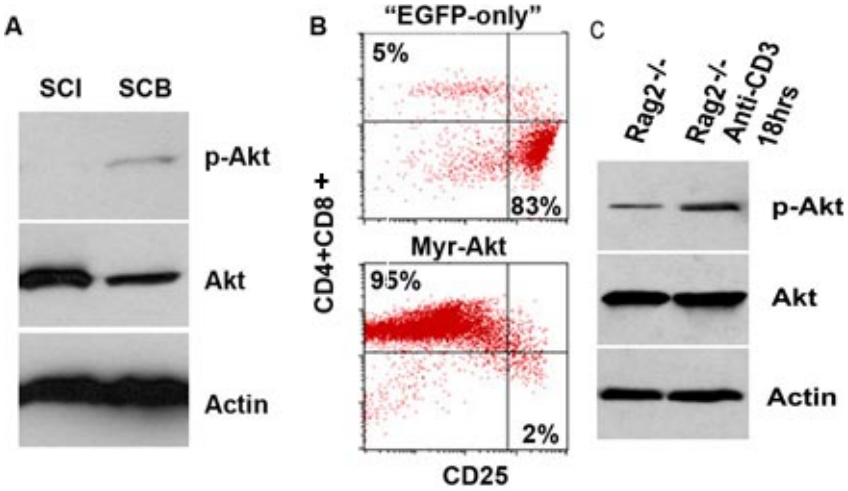

Fig. S4. Akt is downstream of the pre-TCR. (*A*) Comparison of Akt phosphorylation between pre-TCR+ (SCB29) and pre-TCR- parental (SCIET27) cells. Endogenous, total Akt and Actin blots are included as controls. (*B*) Expression of Myr-Akt in Rag-1$^{-/-}$ bone marrow progenitors was able to ''rescue'' the DN to DP arrest. Myr-Akt-expressing (and EFGP-only expressing) progenitors were injected in Rag-2$^{-/-}\gamma c^{-/-}$ hosts and reconstitution was analyzed 6 weeks post transplant. (*C*) RAG2$^{-/-}$ mice were treated with anti-CD3 or an isotype control. Levels of Akt both protein and phosphorylation were assessed at 18 h post injection. Actin was used as a loading control. Data are representative of 2 independent experiments.

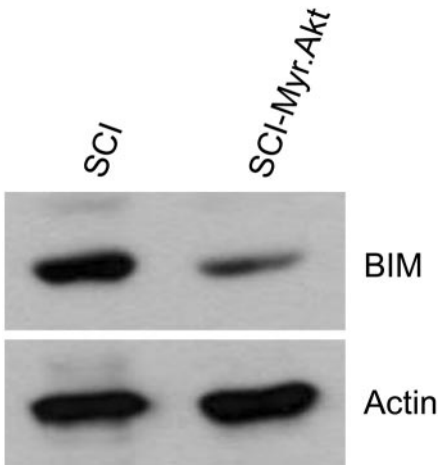

Fig. S5. Comparison of Bim protein expression between pre-TCR- (SCIET27) cells and Myr.Akt expressing SCIET27 cells. Actin blots are included as controls. Data are representative of 2 independent experiments.

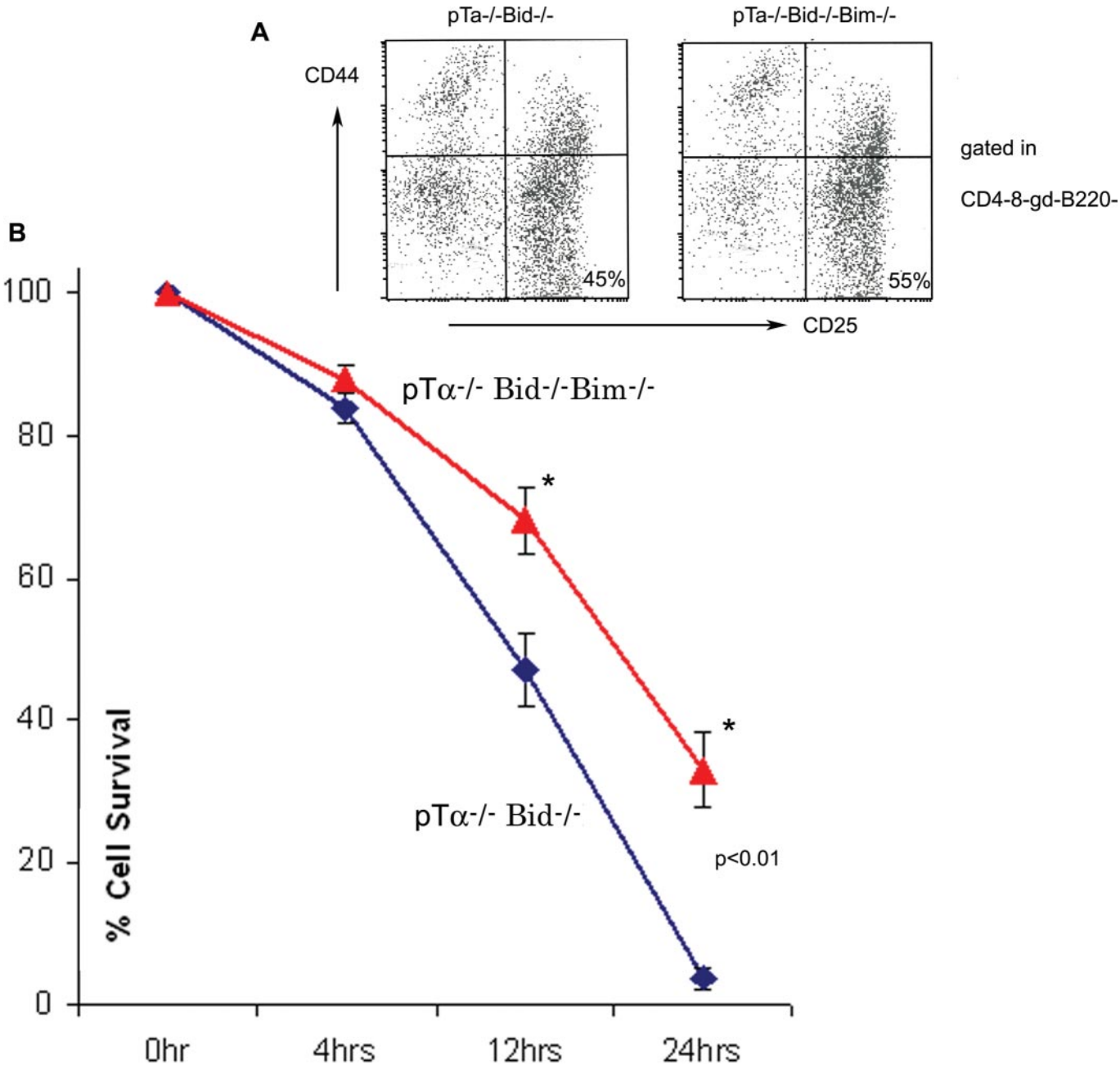

Fig. S6. Bim, Bid and pTα deficiency suppresses pre-T cell death in vivo. (*A*) Phenotypic analysis of total thymocytes by using CD25 and CD44 antibodies. (*B*) DN3 cells from pT$\alpha^{-/-}$BID$^{-/-}$ and pT$\alpha^{-/-}$BID$^{-/-}$ Bim$^{-/-}$ mice were sorted for live cells and cultured in 24-well plates. Thus time 0 was set to 100% to reflect sorted live cells from both populations. Cell viability was analyzed by using Annexin V staining at the indicated time points. Data represent mean ± SD from 4 experimental sets. *, $P < 0.01$.

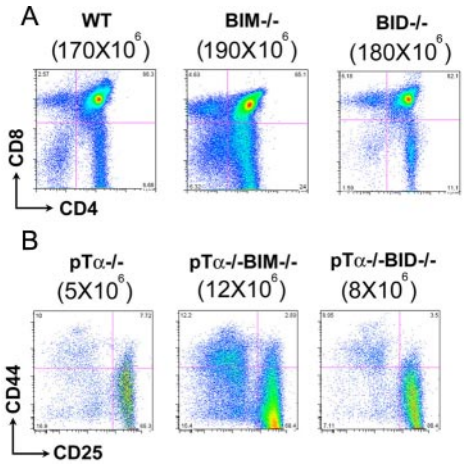

Fig. S7. Phenotypic analysis of pTa$^{-/-}$, pTa$^{-/-}$ × Bid$^{-/-}$ and pTa$^{-/-}$ × Bim$^{-/-}$ thymi. Staining of thymi of the indicated genotypes is shown. (*A*) Total cells, (*B*) CD4^{-}8^{-}gdTCR^{-}CD19^{+} cells. Corresponding absolute thymocyte numbers is also shown.

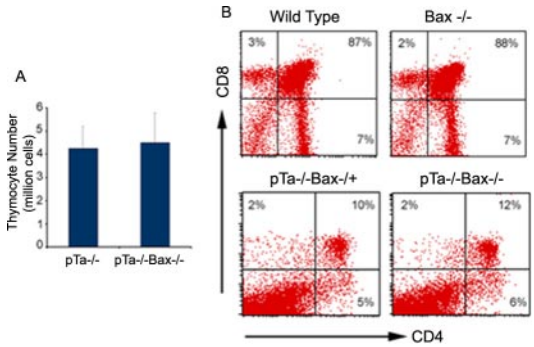

Fig. S8. Phenotypic analysis of pT$\alpha^{-/-} \times$ Bax$^{-/-}$ thymi. (*A*) Comparison of absolute thymocyte numbers purified from pT$\alpha^{-/-}$ and pT$\alpha^{-/-} \times$ Bax$^{-/-}$ littermates. (*B*) CD4 versus CD8 phenotype of littermate mice.

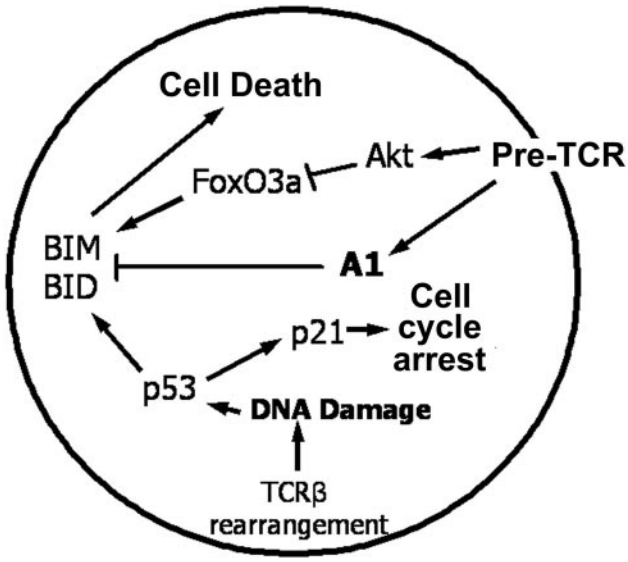

Fig. S9. Working model of regulation of pre-T cell death and survival. Deprivation of trophic signals (IL-7, SCF, pre-TCR) sustain the nuclear localization of FoxO3a which is directly activating the transcription of Bim. TCR VDJ rearrangement is inducing activation of p53, which activates Bid transcription; p53 activation also blocks cell cycle due to its ability to activate the p21 inhibitor. Pre-TCR expression can suppress cell death with at least 2 ways. Initially, it can activate Akt/PKB, phosphorylate FoxO3α inducing its exclusion from the nucleus and thus the silencing of Bim expression. Also, pre-TCR signaling can induce the expression of BCL2A1 (A1), which can bind and inactivate both Bim and Bid proapoptotic activity. Last, the pre-TCR can either directly and/or indirectly suppress p53 activity and Bid expression.

Table S1. Absolute numbers of different thymocyte subsets

1×10^6	WT	pT$\alpha^{-/-}$	pT$\alpha^{-/-}$BIM$^{-/-}$	pT$\alpha^{-/-}$BID$^{-/-}$
	$n = 23$	$n = 18$	$n = 9$	$n = 8$
Total	175.11 ± 21.21	5.75 ± 1.06*	11.21 ± 1.41*,**	7.25 ± 1.06*
CD4$^-$CD8$^-$	6.09 ± 0.74	2.86 ± 0.52*	7.01 ± 0.91**	6.06 ± 0.87***
CD4$^+$CD8$^+$	153.23 ± 18.57	1.36 ± 0.25*	0.81 ± 0.10*,****	0.10 ± 0.01*,***
C4$^+$CD8$^-$	11.67 ± 1.41	0.18 ± 0.03*	0.17 ± 0.02*	0.17 ± 0.03*
CD4$^-$CD8$^+$	3.13 ± 0.38	0.14 ± 0.03*	0.60 ± 0.08*,**	0.05 ± 0.01*,***

Quantitative analysis of thymocytes as determined by flow cytometry. All data are expressed as mean ± SE, which were compared by Student's *t* test. *, $P = 0.001$ as compared with WT; **, $P < 0.001$ as compared with pT$\alpha^{-/-}$; ***, $P < 0.01$ as compared with pT$\alpha^{-/-}$; ****, $P < 0.10$ as compared with pT$\alpha^{-/-}$.